**Oceanologia, 67 (2)/2025, 67204**
**Polish Academy of Sciences**
**Institute of Oceanology**
**Open access article under the CC BY license**
**https://doi.org/10.5607/MSGL7170**

# Thornthwaite method based climate classifying and generation of GIS based climate boundary maps: a case of Kozlu District on the Western Black Sea coast of Turkey

Hulya Keskin Citiroglu[1], Deniz Arca[2,*]

**Abstract**

It is necessary to know the climatic conditions and classes in order to address a region's climate-related problems and ensure its sustainability. Kozlu, located on the Black Sea coast in the Black Sea region of Turkey, is a district where underground mining, fishing, sea tourism and agricultural activities are conducted. The district faces challenges due to geo-environmental factors, including landslides, subsidence, and floods, necessitating the identification of climate classes and characteristics to support sustainable development. For this reason, data for the last thirty years from four meteorological stations representing the Kozlu district were obtained. It was associated with the location, and then the Kriging interpolation method was applied. After this, water balances were calculated by applying the Thornthwaite climate classification method, and GIS-based climate boundary maps were generated using the same method. In the climate classification made by the Thornthwaite method, it was observed that the humid climate characteristic was dominant throughout the district. The drought index indicates moderate summer water deficiency in the north and the south of the district. In the south of the district, it is characterized by little or no water deficiency. Considering that the annual precipitation amounts at the stations located in the south of the district are higher than in the other areas, and the time interval in which water deficiency occurs is shorter, the fact that the climate feature of little or no water deficiency is seen moving south in the study area shows that the results are quite compatible with each other. In addition, according to the results of the summer concentration index, the entire study area was observed to be dominated by a marine climate. Climate boundary maps consisting of precipitation efficiency, temperature efficiency, drought and summer concentration index maps will contribute to monitoring climate change in the district.

**Keywords**

Black Sea coast; Thornthwaite method; Kriging interpolation method; GIS; Climate border map

[1] *Directorate of Aydın Investment Monitoring and Coordination, Aydın YIKOB, Aydın, Turkey*
[2] *Department of Architecture and Urban Planning, Izmir Vocational School, Dokuz Eylul University, Izmir, Turkey*
***Correspondence**: deniz.arca@deu.edu.tr (D. Arca)

**Received**: 17 May 2024; **revised:** 28 January 2025; **accepted**: 3 March 2025

## 1. Introduction

To ensure the sustainability of a region, climatic conditions need to be classified. This classification contributes to works on climate change, irrigation plans and agricultural zoning. Specifying climate catalyzes information sharing for various goals (Rolim et al., 2007). Climate determines the character of the locations in terms of weather events and vegetation. There has been an increase in extreme climatic conditions since the 2000s (Özüpekçe, 2021). Carmin et al. (2012) emphasized that the effects of climate change make living conditions more difficult, especially in the southern hemisphere. The increase in air temperatures leads to increased evaporation. Increased evaporation causes water scarcity. Water scarcity also causes deterioration of vegetation (Orhan et al., 2019). In other words, temperature increase and drought are closely related disasters (Yılmaz, 2023). Heavy or long-term rains are a natural trigger, just like earthquakes (Akinci, 2022).

Global warming, which has accelerated over the last forty years, has led to changes in climate over a wide area (Cui et al., 2021). The Intergovernmental Panel on Climate Change (IPCC) was established in 1988 by the World Meteorological Organization (WMO) and the United Nations Environment Program to assess and understand changes in global climate due to human activities following the Industrial Revolution and to coordinate studies on climate change globally. One of the most important areas of work of the IPCC is the study of alternative situations for the future. Scenarios are stories depicting future events (Gregory and Duran, 2001; Gürkan et al., 2016). A scenario is a description of possible alternative situations (IPCC, 2000). In line with the decisions taken at the 25th Session of the IPCC, a series of resolutions regarding new scenarios was made at the IPCC Experts Meeting held in 2007. In the same meeting, four RCP types were defined in terms of the characteristics determined and the radiative forcing levels and routes. These are RCP3-PD (RCP2.6), RCP4.5, RCP6.0, and RCP8.5, in order from the smallest to largest radiative forcing values. According to the IPCC 5th Assessment Report, temperatures in the Mediterranean basin and Europe will continue to increase throughout the 21st century (IPCC, 2013; Gürkan et al., 2016). The future map is derived from a suite of Phase 5 (CMIP5) model projections under the RCP8.5 scenario (Taylor et al., 2012). Valjarević et al. (2022) analyzed four scenarios regarding climate change in accordance with the TWCC classification in their study, in which they used 4261 meteorological stations from which temperature and precipitation data were taken and two climate models representing the most extreme models in the CMIP6 database. Shanmugam et al. (2024) used the Combined Model Intercomparison Project Phase 6 (CMIP6)-based MIROC6 GCM and SSP245 and SSP585 datasets. With climate change, the summer season has begun to become hotter and drier in regions where the Mediterranean climate prevails (Calda et al., 2020).

As stated in the IPCC reports, Turkey is located in the Eastern Mediterranean basin, which is one of the regions most sensitive to climate change (Gürkan et al., 2016). According to the 2080–2099 period, rainfall anomalies projections for summer and winter made with both CMIP3 and CMIP5, decreases in precipitation are predicted in a large part of Turkey. In the summer season projections, decreases in temperature are predicted for all of Turkey, and increases in temperature are predicted for the coastal parts of the Black Sea Region in the winter (IPCC, 2013; Gürkan et al., 2016). In her study examining the relationship between urban growth and climate change in Yalova province on the coast of the Marmara Sea, Koç (2024) stated that many coastal cities in Turkey are expected to be negatively affected due to sea level rise caused by climate change. To minimize the effects of climate change, it is necessary to ensure the protection of natural areas in Yalova and to take into account possible dangers in the planning of artificial areas (Koç, 2024). In this context, it is necessary to determine climate characters and climate classes. Climate classifications are methods for defining climate patterns (Gallardo et al., 2013; Jacobeit, 2010) and are used to determine seasonal and spatial climate changeability (Bieniek et al., 2012; de Castro et al., 2007). Climate classification systems are used in validating climate models (Jylhä et al., 2010; Belda et al., 2014), in climate change studies (Mahlstein et al., 2013) and in defining agroclimatic zones (Rahimi et al., 2013). There are various climate classification systems such as Holdridge (1967), Flohn (1950), Camargo (1991), Köppen and Geiger (1928) and Thornthwaite (1948). Especially the last two of these methods are the most widely used globally (Spinoni et al., 2014). Climate classification systems play a fundamental role in a variety of fields, from agriculture to urban planning and scientific research, providing an important tool for informed decision-making (Van Delden et al., 2010). Therefore, climate classification contributes significantly to a better understanding and management of climate in different world regions, as well as simplifying the analysis of climatic features (Coumou and Rahmstorf, 2012). The main goal of climate classification is to distinguish different climate kinds and accordingly identify similar or different geographical areas. These classifications are of great importance from a scientific as well as practical perspective. Because the climatic conditions in any geographical area greatly affect almost all studies related to the use of spatial resources in areas such as agriculture, planning, transportation, settlement, and irrigation (Erinç, 1984), it is essential to consider these factors in relevant research.

In the climate classification method proposed by Thornthwaite (1948), climate zones are analyzed by using potential evapotranspiration and water balance elements as well as air temperature and precipitation (Elguindi et al., 2014). Thornthwaite's climate classification plays a fundamental role in determining how plants draw water from the soil and transfer this process to the atmosphere through physiological processes (Bidinger, 1979). This climate classification system is of particular importance when applied for agricultural purposes, and is of particular importance as highlighted by Elguindi et al. (2014). Climate variability inevitably has a direct and significant impact on agricultural production. This has a significant impact on plant growth and productivity.

Thornthwaite (1948) addresses critical aspects such as the relationship between precipitation and soil moisture, surface runoff, and water demand (MGM, 2025). Although the primary purpose of Thornthwaite's (1948) classification is to identify different climate types, it finds extensive practical applications, particularly in areas where evapotranspiration cannot be directly calculated, such as agriculture, hydrogeology, and water resource development. Yalcin and Arca (2024) determined the climate types of Burdur province in Turkey with Köppen, Trewartha, De Martonne, Aydeniz, Erinç and Thornthwaite methods and created their boundary maps. The study emphasized the importance of the Thornthwaite method. In their climate classification studies conducted in Bartın province by Keskin Citiroglu and Arca (2024), in Muğla province by Arca and Keskin Citiroglu (2024), and Safranbolu district by Keskin Citiroglu (2024), various methods were used. They again emphasized that the Thornthwaite method is powerful. De Oliveira Aparecido et al. (2023) conducted climate change analyses using the Thornthwaite method in the state of Maranhão, Brazil, to assess the impacts of climate change on agricultural planning. The study concluded that the decrease in the humidity index would negatively affect various economic activities in Maranhão, such as agriculture, livestock, and fisheries. Santos et al. (2024) applied the Thornthwaite method to predict daily potential evapotranspiration (PET) using a two-grid climate dataset in their study. The results indicated that the Thornthwaite method is a robust approach, as it requires less data compared to other methods and consistently performs well depending on the climate type and dataset used.

It is not likely to quantify meteorological data from all locations in a field, both technically and in terms of cost. For this, climate values on the entire surface must be estimated using interpolation methods to assess the spatial distribution of climate data over several periods. Thus, climate values at other locations can be predicted by using previously measured data. Kozlu district, which was chosen as the study area, is a place where mining, fishing, sea tourism, and agricultural activities are prevalent, and also has development potential. Boz et al. (2020) emphasized in their study the need to create long-term climate maps to ensure sustainability in agriculture. They created maps with long-term humidity, precipitation, and temperature data for the provinces of Bartın, Karabük, Bolu, Zonguldak, and Kastamonu, including the study area of Kozlu. The dependence of cropping systems on rainfall variability will lead to the emergence of climate-resistant agricultural system practices and agricultural policies (Lakshmi et al., 2024). Therefore, determining climate boundaries can help identify agricultural activities and changes in plant species. For these reasons, data for the last thirty years from four meteorological stations in Kozlu district were obtained (Climate Data, 2024). The acquired data were associated with the area, and water balances were calculated by applying the methods of Kriging interpolation (Krige, 1951) and Thornthwaite (1948) climate classification. Later, the climate type was evaluated using the climate classifying method of Thornthwaite (1948) and geographic information systems (GIS)-based climate boundary maps were created. One of the most significant challenges in climate studies today is the lack of a sufficient number of station data. Many meteorological stations are located within cities or along coastlines, resulting in insufficient coverage in high-altitude inland or mountainous regions. This deficiency is being addressed through the use of interpolation techniques aided by computer systems and GIS. Consequently, instead of relying solely on sample points taken along lines in the past, more comprehensive values are now being obtained on a pixel-by-pixel basis. Kriging is an interpolation method that estimates the optimal values of data at other points using data from known nearby points (Yalcin and Arca, 2024).

This study offers an innovation that can be the basis for planning to maintain not only fishing, mining, marine tourism activities and agricultural characteristics of the Kozlu district but also to prevent it from being affected by climate changes. It will also help to examine the possible future alternative situations of Kozlu district due to climate change. Another innovation of this study is the creation of climatic boundary maps using a combined method of Thornthwaite and Kriging interpolation and the GIS for planning. It is thought that this study will guide the evaluations of local authorities regarding Kozlu. In addition, this work aims to help future studies in which Kozlu district public institutions and administrations evaluate water and climate policies together.

## 2. Study area

Kozlu district, which is the closest district of Zonguldak province in the west of the Black Sea region, is located between latitudes from 41 to 27 N. and longitudes from 31 to 49 E. It is 5 km from Zonguldak city centre, 280 km from the capital Ankara, and 326 km from Istanbul. It is surrounded by the Black Sea in the north, Kdz. Ereğli district in the west and south, and Zonguldak province in the east (Figure 1). All neighborhoods of the district, whose center is located at sea level, are located in mountainous areas. It consists of 9 neighborhoods and 24 villages connected to Kozlu Center (Kozlu District Governorship, 2024). Kozlu, which is known for its natural beauties, sea, and cultural values as well as hard coal mining, is a district with high development potential. Ilıksu locality, Değirmenağzı bay and waterfalls, and the coastal road constitute important geographical structures and tourist areas. On the coastline, there are public recreation and sports facilities, fishing shelters, Aqua Park, amusement park, restaurants, astroturf, city stadium, Değirmenağzı and Ilıksu recreational facilities and beaches (Kozlu Municipality, 2024).

The population of Kozlu is 50908 and 43419 of this population lives in the district center. The annual growth rate of the population is 22.7 people per thousand (TUIK, 2024). Boz et al. (2020) emphasized the necessity of making climate maps of this area in their studies in the Western Black Sea region, which includes the Zonguldak province, to which the study area is linked. Bolat et al. (2018) revealed that the amount of precipitation in Zonguldak and its immediate surroundings decreased while the temperature levels increased. Keskin Citiroglu and Baysal (2011) calculated the water balance using the Schendel method (Schendel, 1968) in their study by examining the floods of the Kozlu district. They stated that there is a greater

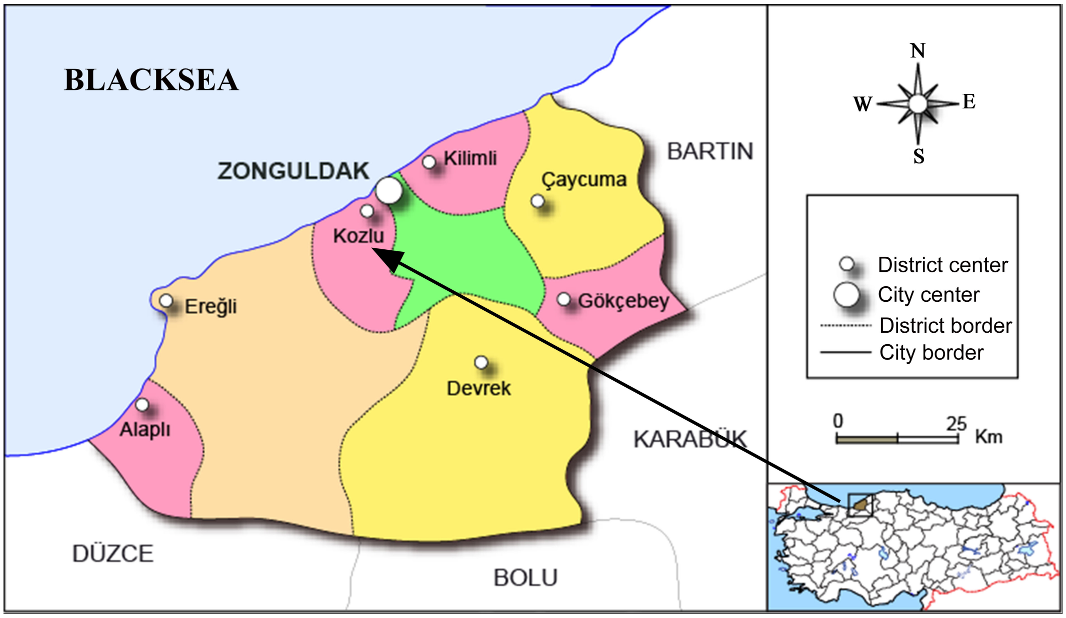


**Figure 1.** Location map (URL-1, 2024).

risk of floods compared to other months, due to the excess water flowing from November to March.

## 3. Material and methods

Calculating water balance with long-term monthly average temperature, precipitation, and evapotranspiration data is necessary for climate classification (Thornthwaite, 1948). Evapotranspiration represents the maximum amount of water that can be lost according to climatic conditions, also known as ETP. The ETP and real evapotranspiration (ETR) values in the Kozlu district have been calculated by the Thornthwaite method (Eq. 1) using monthly average temperature and precipitation data measured at Meteorological Stations, and a GIS-based surface map of climate borders was prepared by applying the Kriging interpolation method (Eq. 2). The Thornthwaite is a method that can reveal both precipitation effectiveness and temperature indices, indicating drought-humidity and maritime-continental contexts. The Thornthwaite method was preferred for the study area because it not only classifies the climate but also reveals the climatic indices and the water balance. Among the various methods, Thornthwaite (1948) was preferred because it can reveal the precipitation efficiency, temperature indices, drought-humidity, and maritime-continental status. With the climate classification, not only were the climate types of the study area determined, but also were the climate boundaries drawn. When many studies using various climatic classifications are examined, the Thornthwaite method is preferred as a method in multiple studies (Yalcin and Arca, 2024; Keskin Citiroglu, 2024; Arca and Keskin Citiroglu, 2024; Keskin Citiroglu and Arca, 2024).

$$\mathrm{ETP} = 16 \times \left(\frac{10 \times t}{I}\right)^{a} \times \ p, \quad i = \left(\frac{t}{5}\right)^{1.514}, \quad I = \sum_{i} \tag{1}$$

$$a = 6.75 \times 10^{-7} \times I^{3} - 7.71 \times 10^{-5} \times I^{2} + 1.79 \times 10^{-2} \times I + 0.49239$$

where ETP is the potential evapotranspiration (mm), t is the average monthly temperature (°C), i is the monthly temperature index, I is the total annual temperature index, and p is the latitude correction coefficient (Thornthwaite, 1948).

$$N_p = \sum_{t=1}^{n} P_i \times N_i \tag{2}$$

In this formula, n represents the number of points, $N_i$ represents the geoid undulation used in the calculation of $N_p$, $N_p$ represents the sought undulation value, and $P_i$ represents the weight associated with each $N_i$ value used in the calculation of N (Krige, 1951; Colak and Memisoglu, 2021).

Using the values in the water balance table, created ETP, excess water and water deficit, the precipitation efficiency index, temperature efficiency index, drought index and summer concentration are calculated to determine the letters reflecting the climate types. Each process step represents a letter of the climate type. Thornthwaite climate classification is carried out in four steps (Thornthwaite, 1948).

In Thornthwaite climate classification, the first letter represents the precipitation efficiency index value and is obtained using the formula ($I_m$) (Thornthwaite 1948) (Eq. 3). In this formula, (s) represents the annual excess water, and (d) represents the annual water deficit.

$$I_m = \frac{100 \times s - 60 \times d}{ETP} \quad (3)$$

The second letter in the Thornthwaite climate classification constitutes the Thornthwaite temperature efficiency index. This value is determined based on the annual ETP values (Thornthwaite, 1948). The third letter in the Thornthwaite classification constitutes the precipitation regime indices. The precipitation regime indices are as follows: aridity index ($I_a$) for rainy climates (Eq. 4) (Thornthwaite, 1948).

$$I_a = \frac{100 \times d}{n} \quad (4)$$

where $I_a$ indicates drought index for wet climates, d annual water deficit, and n annual ETP.

The fourth letter of the climate types in the Thornthwaite classification is determined by the ratio of the ETP in the summer months to the annual ETP. The three summer months here represent the annual temperature rates for the months of June, July and August. The index reflecting the efficiency of temperature concentration during summer yields the climatic characteristic (Thornthwaite, 1948).

With the advancement of technology, conducting spatial analyses using statistical and geographic programs to determine the current situation and take precautions against future conditions has become crucial. Spatial analyses are facilitated by GIS programs (Arslan, 2021). GIS; organized to dissolve complex projection and management problems; It is a framework of hardware, software and methods that covers the processes of covering, managing, processing, analyzing, modeling and displaying data whose location is determined in space (Işlem GIS, 2005). Software systems, as in all fields, also provide opportunities for climate classification. The final maps created through these and similar systems support current data by closely approximating real values. Through the spatial analysis plugin available in GIS software used to obtain data for unknown regions from known point data, it has become possible to generate a continuous surface that represents climate data for the investigated area (Singh and Khan, 2011). For this purpose, spatial maps have been generated using the Kriging interpolation method within a GIS environment. In the Kriging method, a variance value is calculated for each point, which is crucial for the reliability of the models. The Kriging interpolation method was enhanced by mining engineer Danie Gerhardus Krige (Üstüntaş, 2006). Kriging refers to a series of interpolation methods for estimating values at unobserved locations. The location is estimated by a linear combination of values at surrounding locations using weights (Bostan, 2017). The difference between the Kriging method and other interpolation methods is its ability to calculate a variance value for each location being forecasted. This also increases the credibility of the obtained values (Yaprak and Arslan, 2008). Kriging is used for advanced forecast surface modeling and also accounts for errors or prediction uncertainty (Bajjali, 2017). The Kriging method, while supplying more certain crops in proportion to other methods, also helps find minimum variance and the normal deviation of the estimate (Taylan and Damçayırı, 2016). The variance value obtained through the method is called the Kriging variance (Krige, 1951). Kriging methods include various techniques such as Ordinary Kriging, Universal Kriging, Co-Kriging, and Indicator Kriging (Aalto et al., 2013). The choice of the method to be used depends on the characteristics of the data and the type of model desired. In this study, Ordinary Kriging was selected for the analysis of climate data. In the Kriging method, before performing geostatistical estimation, a variogram is calculated based on the distances between sample pairs. The most commonly used variogram models are spherical, exponential, and Gaussian functions (Uyan and Cay, 2013). The optimal variogram model is chosen through trial and error based on the highest correlation coefficient (Uyan and Cay, 2013). The semivariogram, a core component of Kriging, is an effective tool for assessing spatial variability. It provides a clear definition of the spatial structure of variables and offers insight into the processes that may influence the data distribution (Behera and Shukla, 2015). In this study, the Spherical variogram model was chosen due to its suitability for the spatial structure of the data, its ability to provide more accurate predictions, and its practical advantages in terms of computation.

In this study, the climate data for the last thirty years of the Kozlu district were first recorded, and meteorological station points that would best represent the district were identified. For this purpose, meteorological stations located in the Kozlu, Kozluköy, Enseköy, and Sakaköy locations of the Kozlu district were selected (Table 1).

The locational distribution of the stations within the district was taken into consideration when selecting the stations. Kozlu station is located in the north of the district, close to the Black Sea coast, and represents the area due to the influence of the sea. Kozluköy station represents the east of the district, and Sakaköy station represents the west. Kozluköy station also ranks second in terms of proximity to the Black Sea. Enseköy station is located at the very southern end of the district and is the station farthest from the Black Sea coast. The data used in the study were obtained through Climate Data (2024). First, the meteorological station points that recorded the climate data for the last thirty years in Kozlu were determined. For this pur-

**Table 1.** Information of stations

| Stations | Altitude (m) | Latitude (N) | Longitude(E) | Period (year) |
|---|---|---|---|---|
| Kozlu | 147 | 41°26′19.86″ | 31°45′14.33″ | 1991–2021 |
| Kozluköy | 290 | 41°24′3.6″ | 31°45′24.2″ | 1991–2021 |
| Enseköy | 353 | 41°17′8.12″ | 31°46′43.17″ | 1991–2021 |
| Sakaköy | 363 | 41°21′12.09″ | 31°40′32.18″ | 1991–2021 |

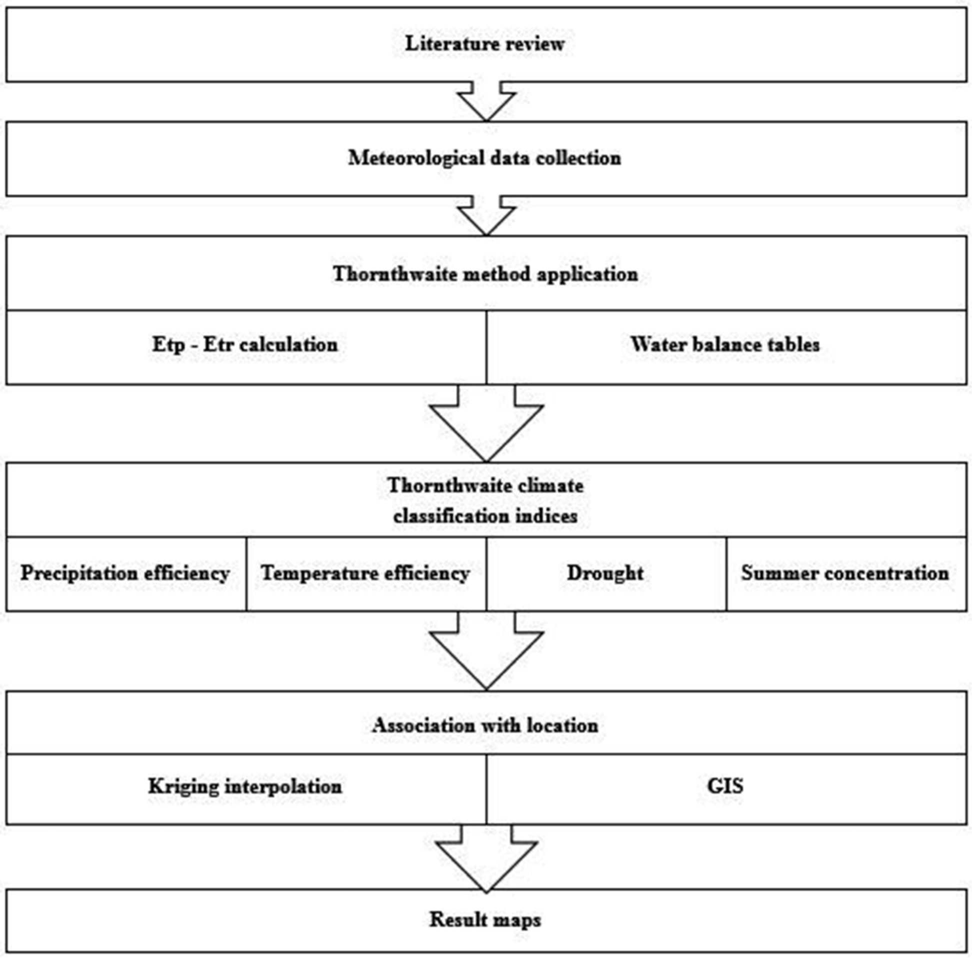


**Figure 2.** Flowchart of the study.

pose, the meteorological station points located in Kozlu, Kozluköy, Enseköy, and Sakaköy in the Kozlu district were selected. The data were arranged for all meteorological station points in order to associate them with the location. The location information of all stations was associated with the information obtained from Climate Data (2024) and thus it was transferred to the geographic database and made available for analysis. (Figure 2) shows a flowchart diagram.

## 4. Results and discussion

To accurately represent the climate characteristics of Kozlu, data from four meteorological stations were utilized, covering the entire district (Climate Data, 2024). Climate diagrams prepared using long-term average precipitation and temperature data for all stations are depicted in (Figure 3), while the climograms are shown in (Figure 4).

From meteorological data spanning the last 30 years, it is observed that precipitation occurs in all months in the Kozlu district. However, in October, an increase in precipitation begins that will last for approximately four months. The annual amount of precipitation at Enseköy and Sakaköy stations is higher than at other stations. The annual total precipitation height is 1037 mm in the western and southern parts of the investigated area, and 915 mm in the northern and eastern parts. As you move towards the south of the study area, an increase in precipitation amount is observed. The annual precipitation height being

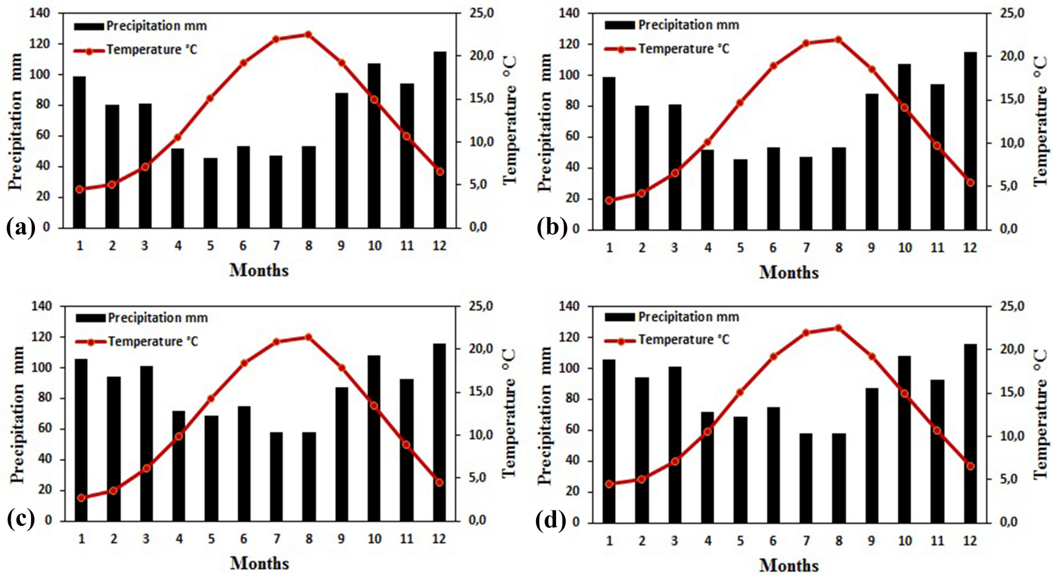


**Figure 3.** Climate diagrams. Kozlu (a), Kozluköy (b), Enseköy (c), Sakaköy (d).

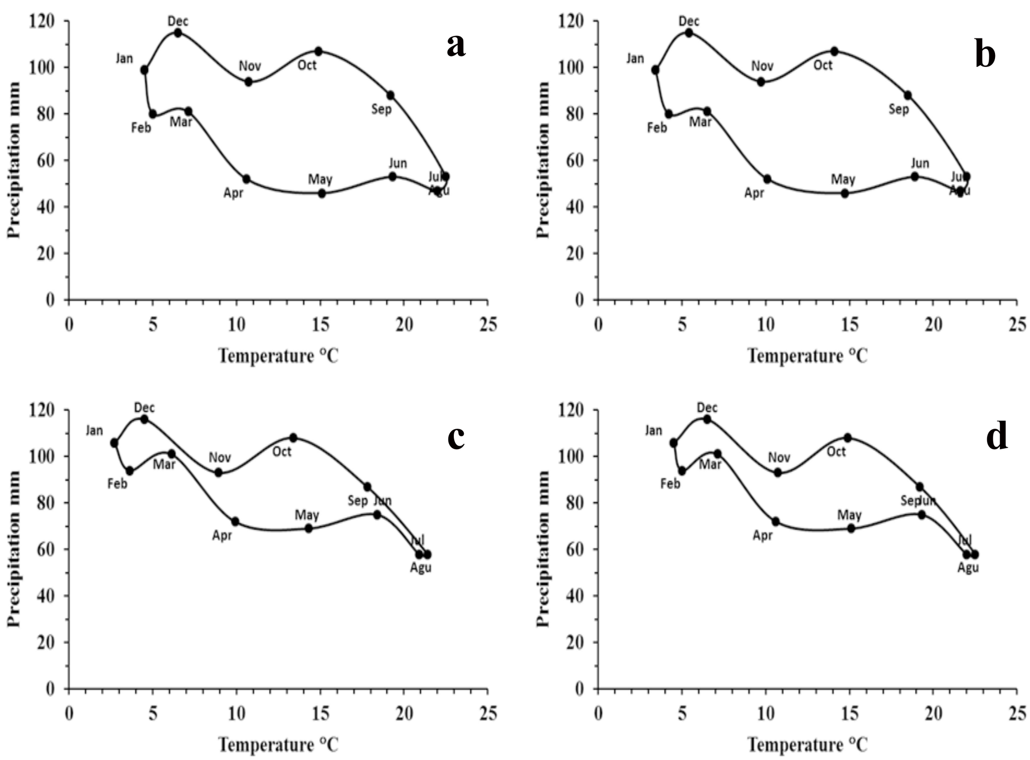


**Figure 4.** Climograms. a) Kozlu, b) Kozluköy, c) Enseköy, d) Sakaköy.

**Table 2.** Water balance of Kozlu station.

| Kozlu | 1 | 2 | 3 | 4 | 5 | 6 | 7 | 8 | 9 | 10 | 11 | 12 | Annual |
|---|---|---|---|---|---|---|---|---|---|---|---|---|---|
| Precipitation | 99 | 80 | 81 | 52 | 46 | 53 | 47 | 53 | 88 | 107 | 94 | 115 | 915 |
| Temperature C° | 4.5 | 5 | 7.1 | 10.6 | 15.1 | 19.3 | 22 | 22.5 | 19.2 | 14.9 | 10.7 | 6.5 | 13.1 |
| Max. Temp. C° | 7.2 | 7.9 | 10.1 | 13.5 | 17.7 | 21.8 | 24.5 | 25.1 | 21.9 | 17.5 | 13.7 | 9.3 | 15.9 |
| Rel. Humidity % | 78 | 77 | 75 | 77 | 80 | 79 | 79 | 78 | 78 | 79 | 77 | 78 | 78 |
| Monthly t. index i | 0.853 | 1.000 | 1.700 | 3.119 | 5.330 | 7.728 | 9.423 | 9.749 | 7.668 | 5.224 | 3.164 | 1.488 | 56.446 |
| Lat. Correction | 0.83 | 0.83 | 1.03 | 1.11 | 1.25 | 1.26 | 1.27 | 1.19 | 1.04 | 0.96 | 0.82 | 0.80 | – |
| ETP mm | 11.7 | 13.5 | 22.0 | 38.1 | 62.1 | 87.1 | 104.4 | 107.6 | 86.5 | 61.0 | 38.6 | 19.4 | 652.1 |
| Corrected ETP | 9.7 | 11.2 | 22.6 | 42.3 | 77.6 | 109.8 | 132.5 | 128.1 | 90.0 | 58.5 | 31.7 | 15.5 | 729.7 |
| P-ETP mm | 89.3 | 68.8 | 58.4 | 9.7 | −31.6 | −56.8 | −85.5 | −75.1 | −2.0 | 48.5 | 62.3 | 99.5 | 185.3 |
| Reserve water | 100 | 100 | 100 | 100 | 68.4 | 11.6 | 00 | 00 | 00 | 48.5 | 100 | 100 | – |
| ETR mm | 9.7 | 11.2 | 22.6 | 42.3 | 77.6 | 109.8 | 58.6 | 53 | 88 | 58.5 | 31.7 | 15.5 | 578.5 |
| Water deficit | 00 | 00 | 00 | 00 | 00 | 00 | 73.9 | 75.1 | 2 | 00 | 00 | 00 | 151 |
| Excess water | 89.3 | 68.8 | 58.4 | 9.7 | 00 | 00 | 00 | 00 | 00 | 00 | 10.8 | 99.5 | 336.5 |
| Runoff mm | 44.7 | 56.8 | 46.4 | 19.5 | 2.4 | 00 | 00 | 00 | 00 | 00 | 5.4 | 52.5 | 227.71 |

**Table 3.** Water balance of Kozluköy station.

| Kozluköy | 1 | 2 | 3 | 4 | 5 | 6 | 7 | 8 | 9 | 10 | 11 | 12 | Annual |
|---|---|---|---|---|---|---|---|---|---|---|---|---|---|
| Precipitation | 99 | 80 | 81 | 52 | 46 | 53 | 47 | 53 | 88 | 107 | 94 | 115 | 915 |
| Temperature C° | 3.4 | 4.2 | 6.5 | 10.1 | 14.7 | 18.9 | 21.6 | 22 | 18.5 | 14.1 | 9.7 | 5.4 | 12.4 |
| Max. Temp. C° | 6.7 | 7.7 | 10.1 | 13.8 | 18 | 22 | 24.7 | 25.3 | 21.9 | 17.4 | 13.4 | 8.8 | 15.8 |
| Rel. Humidity % | 79 | 77 | 75 | 77 | 79 | 78 | 77 | 76 | 77 | 79 | 78 | 79 | 78 |
| Montly t. index i | 0.558 | 0.768 | 1.488 | 2.899 | 5.118 | 7.487 | 9.165 | 9.423 | 7.249 | 4.805 | 2.727 | 1.124 | 52.810 |
| Lat. Correction | 0.83 | 0.83 | 1.03 | 1.11 | 1.25 | 1.26 | 1.27 | 1.19 | 1.04 | 0.96 | 0.82 | 0.80 | – |
| ETP mm | 8.9 | 11.8 | 21.1 | 37.7 | 61.9 | 86.3 | 103.0 | 105.5 | 83.9 | 58.6 | 35.7 | 16.5 | 631.1 |
| Corrected ETP | 7.4 | 9.8 | 21.7 | 41.9 | 77.4 | 108.8 | 130.8 | 125.6 | 87.3 | 56.3 | 29.3 | 13.2 | 709.4 |
| P-ETP mm | 91.6 | 70.2 | 59.3 | 10.1 | −31.4 | −55.8 | −83.8 | −72.6 | 0.7 | 50.7 | 64.7 | 101.8 | 205.6 |
| Reserve water | 100 | 100 | 100 | 100 | 68.6 | 12.8 | 00 | 00 | 0.7 | 51.4 | 100 | 100 – | |
| ETR mm | 7.4 | 9.8 | 21.7 | 41.9 | 77.4 | 108.8 | 59.8 | 53 | 87.3 | 56.3 | 29.3 | 13.2 | 565.9 |
| Water deficit | 00 | 00 | 00 | 00 | 00 | 00 | 71 | 72.6 | 00 | 00 | 00 | 00 | 143.6 |
| Excess water | 91.6 | 70.2 | 59.3 | 10.1 | 00 | 00 | 00 | 00 | 00 | 00 | 16.1 | 101.8 | 349.1 |
| Runoff mm | 45.8 | 58 | 47.2 | 19.9 | 2.5 | 00 | 00 | 00 | 00 | 00 | 8.1 | 54.9 | 236.4 |

**Table 4.** Water balance of Enseköy station.

| Enseköy | 1 | 2 | 3 | 4 | 5 | 6 | 7 | 8 | 9 | 10 | 11 | 12 | Annual |
|---|---|---|---|---|---|---|---|---|---|---|---|---|---|
| Precipitation | 106 | 94 | 101 | 72 | 69 | 75 | 58 | 58 | 87 | 108 | 93 | 116 | 1037 |
| Temperature °C | 2.7 | 3.6 | 6.1 | 9.9 | 14.3 | 18.4 | 20.9 | 21.4 | 17.8 | 13.4 | 8.9 | 4.5 | 11.8 |
| Max. Temp. °C | 6.2 | 7.4 | 10 | 13.9 | 18 | 21.8 | 24.4 | 25 | 21.6 | 17.1 | 13.1 | 8.3 | 15.6 |
| Rel. Humidity % | 79 | 77 | 76 | 77 | 78 | 78 | 77 | 76 | 78 | 79 | 78 | 79 | 78 |
| Monthly t. index i | 0.393 | 0.608 | 1.351 | 2.813 | 4.908 | 7.189 | 8.719 | 9.037 | 6.837 | 4.448 | 2.394 | 0.853 | 49.551 |
| Lat. Correction | 0.83 | 0.83 | 1.03 | 1.11 | 1.25 | 1.26 | 1.27 | 1.19 | 1.04 | 0.96 | 0.82 | 0.80 | – |
| ETP mm | 7.4 | 10.7 | 20.8 | 38.6 | 61.6 | 84.9 | 99.8 | 102.9 | 81.4 | 56.7 | 33.7 | 14.2 | 612.7 |
| Corrected ETP | 6.1 | 8.8 | 21.5 | 42.8 | 77.0 | 107.0 | 126.8 | 122.4 | 84.7 | 54.5 | 27.6 | 11.3 | 690.6 |
| P-ETP mm | 99.9 | 85.2 | 79.5 | 29.2 | −8.0 | −32.0 | −68.8 | −64.4 | 2.3 | 53.5 | 65.4 | 104.7 | 346.4 |
| Reserve water | 100 | 100 | 100 | 100 | 92 | 60 | 00 | 00 | 2.3 | 55.8 | 100 | 100 | – |
| ETR mm | 6.1 | 8.8 | 21.5 | 42.8 | 77 | 107 | 118 | 58 | 84.7 | 54.5 | 27.6 | 11.3 | 617.3 |
| Water deficit | 00 | 00 | 00 | 00 | 00 | 00 | 8.8 | 64.4 | 00 | 00 | 00 | 00 | 73.2 |
| Excess water | 99.9 | 85.2 | 79.5 | 29.2 | 00 | 00 | 00 | 00 | 00 | 00 | 21.2 | 104.7 | 419.7 |
| Runoff mm | 50 | 67.6 | 61.1 | 34.5 | 7.3 | 00 | 00 | 00 | 00 | 00 | 10.6 | 57.7 | 288.8 |

close to 1000 mm indicates that plants' water needs can be met through rainfall, and dry farming can be practiced without the need for artificial irrigation. In the region, October and December receive more precipitation compared

**Table 5.** Water balance of Sakaköy station

| Sakaköy | 1 | 2 | 3 | 4 | 5 | 6 | 7 | 8 | 9 | 10 | 11 | 12 | Annual |
|---|---|---|---|---|---|---|---|---|---|---|---|---|---|
| Precipitation | 106 | 94 | 101 | 72 | 69 | 75 | 58 | 58 | 87 | 108 | 93 | 116 | 1037 |
| Temperature °C | 4.5 | 5 | 7.1 | 10.6 | 15.1 | 19.3 | 22 | 22.5 | 19.2 | 14.9 | 10.7 | 6.5 | 13.1 |
| Max. Temp. °C | 7.2 | 7.9 | 10.1 | 13.5 | 17.7 | 21.8 | 24.5 | 25.1 | 21.9 | 17.5 | 13.7 | 9.3 | 15.9 |
| Rel. Humidity % | 78 | 77 | 75 | 77 | 80 | 79 | 79 | 78 | 78 | 79 | 77 | 78 | 78 |
| Monthly t. index i | 0.853 | 1.000 | 1.700 | 3.119 | 5.330 | 7.728 | 9.423 | 9.749 | 7.668 | 5.224 | 3.164 | 1.488 | 56.446 |
| Lat. Correction | 0.83 | 0.83 | 1.03 | 1.11 | 1.25 | 1.26 | 1.27 | 1.19 | 1.04 | 0.96 | 0.82 | 0.80 | – |
| ETP mm | 11.7 | 13.5 | 22.0 | 38.1 | 62.1 | 87.1 | 104.4 | 107.6 | 86.5 | 61.0 | 38.6 | 19.4 | 652.1 |
| Corrected ETP | 9.7 | 11.2 | 22.6 | 42.3 | 77.6 | 109.8 | 132.5 | 128.1 | 90.0 | 58.5 | 31.7 | 15.5 | 729.7 |
| P-ETP mm | 96.3 | 82.8 | 78.4 | 29.7 | −8.6 | −34.8 | −74.5 | −70.1 | −3.0 | 49.5 | 61.3 | 100.5 | 307.3 |
| Reserve water | 100 | 100 | 100 | 100 | 91.4 | 56.6 | 00 | 00 | 00 | 49.5 | 100 | 100 | – |
| ETR mm | 9.7 | 11.2 | 22.6 | 42.3 | 77.6 | 109.8 | 114.6 | 58 | 87 | 58.5 | 31.7 | 15.5 | 638.5 |
| Water deficit | 00 | 00 | 00 | 00 | 00 | 00 | 17.9 | 70.1 | 3 | 00 | 00 | 00 | 91 |
| Excess water | 96.3 | 82.8 | 78.4 | 29.7 | 00 | 00 | 00 | 00 | 00 | 00 | 10.8 | 100.5 | 398.5 |
| Runoff mm | 48.2 | 65.5 | 59.9 | 34.5 | 7.4 | 00 | 00 | 00 | 00 | 00 | 5.4 | 53 | 273.9 |

to other months. The average highest temperatures are observed throughout the study area in July and August, while the average minimum temperatures occur in January and February (Figure 3). The temperature in Kozlu shows a decreasing trend in September and begins to rise again from April. From the diagram shown in Figure 3, Kozlu is observed to have meteorological characteristics with no significant differences between seasons. The closed shape that appears in Figure 4 shows that the northern part of the Kozlu district, i.e., on the Black Sea coast and near the shore, has a climate type that does not differ much between the seasons in terms of temperature and precipitation. The southern part of the Kozlu district, reflects the climatic characteristics that are slightly different between the seasons in terms of precipitation and temperature compared to the north.

Calculations have been made to produce the water balance of the Kozlu district, and water balances were calculated according to the Thornthwaite method (Thornthwaite, 1948) of the meteorological station data of Kozlu (Table 2), Kozluköy (Table 3), Enseköy (Table 4) and Sakaköy (Table 5).

According to the Thornthwaite method and based on the data from the Kozlu station located in the north of the investigated area, the annual precipitation of 915 mm, 729.7 mm, or 79.8% returns to the atmosphere through evapotranspiration. Considering that the total annual runoff is 227.7 mm, 24.9% of the precipitation contributes to surface runoff. After subtracting the excess water from surface runoff, the remaining 108.8 mm, or 11.9% of the annual total precipitation, infiltrates into the soil. An examination of the monthly variation graph of precipitation and ETP (Figure 5a), reveals that there is an ETP deficit. ETP is greater than ETR during the July to September drought period due to the lack of soil moisture. From October to May, precipitation exceeds ETP. Soil moisture reserves are depleted from late May to November. The water deficit in July, August, and September is 151 mm. This term requires irrigation in agricultural fields. During the rainy season from October to July, the soil is fully or partially saturated, so the ETP amount can be met from soil moisture and precipitation, making ETP equal to ETR during this period. The excess water during this period totals 336.5 mm, which is 36.8% of the total precipitation.

According to the Thornthwaite method, based on the data from the Kozluköy station representing the western part of the study area, 709.4 mm, or 77.5% of the annual precipitation of 915 mm, returns to the atmosphere through evapotranspiration. Considering that the total annual runoff is 236.4 mm, 25.8% of the precipitation contributes to surface runoff. After subtracting the excess surface runoff, the remaining 112.7 mm, or 12.3% of the total annual precipitation, infiltrates into the soil. Examining the monthly variation graph of precipitation and evapotranspiration (Figure 5b), indicates that there is an evapotranspiration deficit. During the dry period comprising July and August, the ETP exceeds the ETR due to the absence of soil moisture. From September to May, precipitation exceeds ETP. From late May to late October, soil moisture reserves are depleted. During July and August, the water deficit amounts to 143.6 mm, coinciding with the months when irrigation is necessary in agricultural areas. In the period from September to July, constituting the rainy season, the soil is either fully or partially saturated with water. Therefore, the amount of ETP can be met from soil moisture and rainfall, making ETP equal to ETR during this term. During this time, the excess water amounts to 349.1 mm annually, which is equivalent to 38.2% of the total precipitation.

According to the Thornthwaite method, based on the data from the Enseköy station located in the southern part of the study area, 690.6 mm, or 66.6% of the annual precipitation of 1037 mm, returns to the atmosphere through evapotranspiration. Considering that the total annual runoff is 288.8 mm, we observe that 27.9% of the

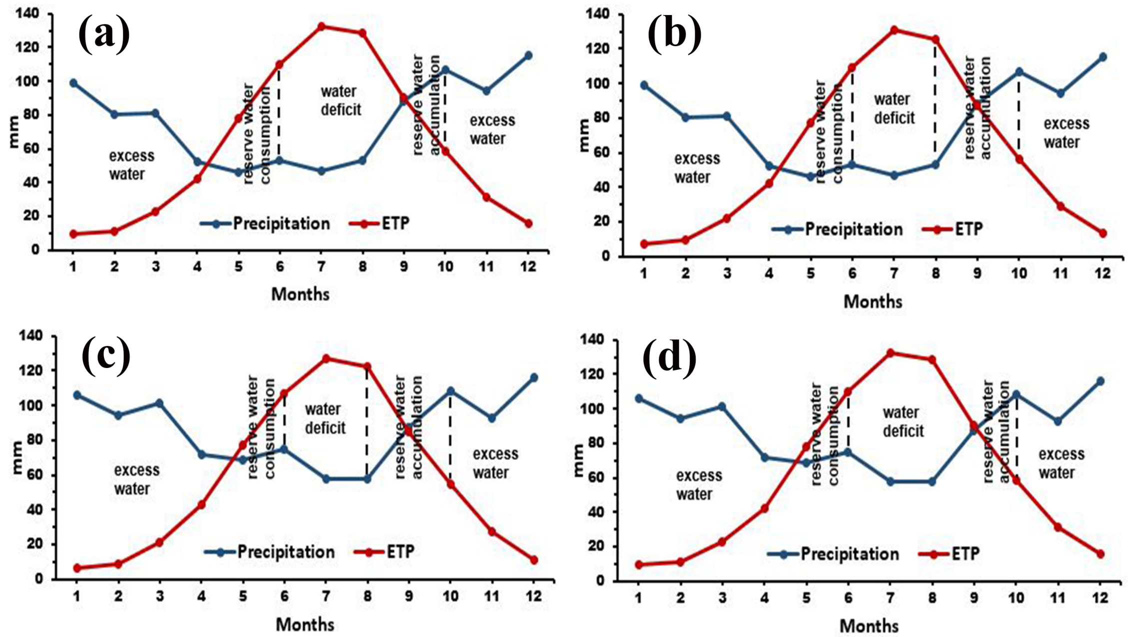


**Figure 5.** Monthly relationship graphs between ETP and precipitation: Kozlu (a), Kozluköy (b), Enseköy (c), Sakaköy (d).

**Table 6.** Climate classification of Kozlu district.

| Stations | Method | | | |
|---|---|---|---|---|
| | Thornthwaite | | | |
| | 1. | 2. | 3. | 4. |
| Kozlu | Humid (B1) | 2nd Degree Mesothermal (B'2) | Moderate summer water deficiency (s) | Marine (b'4) |
| Kozluköy | Humid (B1) | 1st Degree Mesothermal (B'1) | Moderate summer water deficiency (s) | Marine (b'4) |
| Enseköy | Humid (B2) | 1st Degree Mesothermal (B'1) | Little or no water deficiency (r) | Marine (b'4) |
| Sakaköy | Humid (B2) | 2nd Degree Mesothermal (B'2) | Little or no water deficiency (r) | Marine (b'4) |

precipitation contributes to surface runoff. After subtracting the excess surface runoff, the remaining 130.9 mm, or 12.6% of the total annual precipitation, infiltrates into the soil. Examining the monthly variation graph of precipitation and evapotranspiration (Figure 5c), shows an ETP deficit. During the dry period comprising July and August, the ETP exceeds the ETR due to the absence of soil moisture. From September to May, precipitation exceeds ETP. From late May to November, soil moisture reserves are depleted. The water deficit during July and August amounts to 73.2 mm, necessitating irrigation in agricultural areas during these months. During the rainy season typically from April to September, the soil is either fully saturated or partially saturated with water, allowing the ETP to be met from soil moisture and precipitation, making ETP equal to reference ETR during this term. The excess water during this time totals 419.7 mm annually, which is equivalent to 40.5% of the total precipitation.

According to the Thornthwaite method, based on the data from the Sakaköy station representing the eastern part of the study area, 729.7 mm, or 70.4% of the annual precipitation of 1037 mm, returns to the atmosphere through evapotranspiration. Considering that the total annual runoff is 273.9 mm, it can be observed that 26.4% of the precipitation contributes to surface runoff. After subtracting the excess surface runoff, the remaining 124.6 mm, or 12% of the total annual precipitation, infiltrates into the soil. Examining the monthly variation graph of precipitation and evapotranspiration (Figure 5d), one can observe an evapotranspiration deficit. During the dry period comprising July, August, and September, the ETP exceeds the reference ETR due to the absence of soil moisture. From October to May, precipitation exceeds ETP. From late May to late October, soil moisture reserves are depleted. The water deficit during July, August, and September amounts to 91 mm, necessitating irrigation in agricultural areas during these months. During the rainy season from October to August, the soil is either fully saturated or partially saturated with water, allowing the ETP to be met from soil moisture and precipitation, which makes ETP equal to ETR during this period. The excess water during this time totals 398.5 mm annually, which is equivalent to 38.4% of the total precipitation.

As one moves southward in the Kozlu district, the annual rainfall increases, while the intensity and duration of high temperatures and periods of water deficit decrease. Throughout Kozlu, ETP is highest in July and lowest in January. ETR, on the other hand, is lowest in January throughout the district, while it reaches its peak in June for Kozlu and Kozluköy stations and in July for Enseköy and Sakaköy stations. Additionally, from November to May, there is excess water and surface runoff throughout the district. Some of the excess water contributes to surface runoff, while some infiltrates into the soil, with the peak surface runoff occurring in February. It was observed that as we moved south in Kozlu, there was an increase in the amount of runoff with precipitation, and a decrease in the ETP, water deficit amounts, and the time interval during which water deficit was observed with temperature. In Kozlu, steep areas with a slope of 30–40% cover a large area, areas with a slope of 40–60% constitute the mountainous regions in the north of the study area. Coastal plains and valley floors include areas with a slope of 0–30%, and sea cliffs with a slope of 70–90% cover a small area (Arca et al., 2017). In Kozlu, steep areas with a slope of 30–40% cover a large area, while areas with a slope of 40–60% constitute the mountainous regions in the north of the study area. Coastal plains and valley floors include areas with a slope of 0–30%, while sea cliffs with a slope of 70–90% cover a small area (Arca et al., 2017). When the Kozlu slope map and land use map (Arca and Keskin Citiroglu, 2022) were examined, no significant relationship was found between the amount of precipitation and the slope. There was an increase in the amount of precipitation and a decrease in the annual average temperature as we moved away from the Black Sea coast.

A Kruskal-Wallis test was applied to determine whether the potential differences in the ETP values measured by the four stations were random or statistically significant. The Kruskal-Wallis test is a non-parametric test used to assess whether the observed variation in different samples is due to random error or represents a real difference caused by the samples coming from different populations (Schmidt, 2010). The p-value obtained from the Kruskal-Wallis test was 0.914008, which is greater than 0.05. Therefore, it was concluded that there is no statistically significant difference between the ETP values. This finding indicates that the ETP values measured at the four stations reflect similar seasonal conditions and that no statistically significant difference exists between them.

The Thornthwaite method was used to assess precipitation patterns, determine the climate type in the Kozlu district, and create climate boundary maps (Table 6).

Based on the Thornthwaite climate classification method using data from the Kozlu point, the precipitation efficiency index ($I_m$) was determined as 33.7, indicating a Moist (B1) climate characteristic. The Thornthwaite temperature efficiency index, defined based on annual ETP of 729.7 mm, yields a climate characteristic of Second Degree Mesothermal Moist (B’2). The Thornthwaite drought index ($I_a$) was detemined as 20.7, corresponding to a climate characteristic of moderate summer water deficiency (s). The summer concentration index is 50.8%, indicating marine areas (b’4).

Using data from the Kozluköy point, the precipitation efficiency index ($I_m$) was calculated as 37.1 based on the Thornthwaite climate classification method, indicating a Moist (B1) climate characteristic. The Thornthwaite temperature efficiency index, defined based on the annual ETP of 709.4 mm, yields a climate characteristic of First Degree Mesothermal Moist (B’1). The Thornthwaite drought index ($I_a$) was calculated to be 20.2, corresponding to a climate characteristic of moderate summer water deficiency (s). The summer concentration index is 51.5%, which indicates marine areas (b’4).

Based on the Thornthwaite climate classification method using data from the Enseköy point, the precipitation efficiency index ($I_m$) was calculated as 54.4, indicating a Moist (B2) climate characteristic. The Thornthwaite temperature efficiency index, defined based on the annual ETP of 690.6 mm, yields a climate characteristic of First Degree Mesothermal Moist (B’1). The Thornthwaite drought index ($I_a$) was calculated as a value of 10.6, corresponding to a climate feature of little or no water deficiency (r). The summer concentration index is 51.6%, indicating marine areas (b’4).

Based on the Thornthwaite climate classification method using data from the Sakaköy point, the precipitation efficiency index ($I_m$) was detemined as 47.1, indicating a Moist (B2) climate feature. The Thornthwaite temperature efficiency index, determined based on annual ETP of 729.7 mm, yields a climate characteristic of Second Degree Mesothermal Moist (B’2). The Thornthwaite drought index ($I_a$) was calculated as 12.5, corresponding to a climate characteristic of little or no water deficiency (r). The summer concentration index is 50.8%, indicating marine areas (b’4).

According to the climate characteristic represented by the first and second letters obtained in the climate classification made by the Thornthwaite method, it has been observed that the humid climate characteristic is dominant throughout the district. The third letter representing the drought index for rainy climates indicates moderate summer water deficiency for Kozlu and Kozluköy stations, while Enseköy and Sakaköy stations exhibit little or no water deficiency. As one moves southward in the study area, precipitation increases, average temperatures slightly decrease, and the duration of water deficit diminishes. Therefore, it can be concluded that as one moves southward in the study area, a climate characterized by little or no water deficiency is observed. Additionally, based on the results of the summer concentration index represented by the fourth letter in the Thornthwaite method, it is observed that the entire Kozlu district exhibits a marine climate.

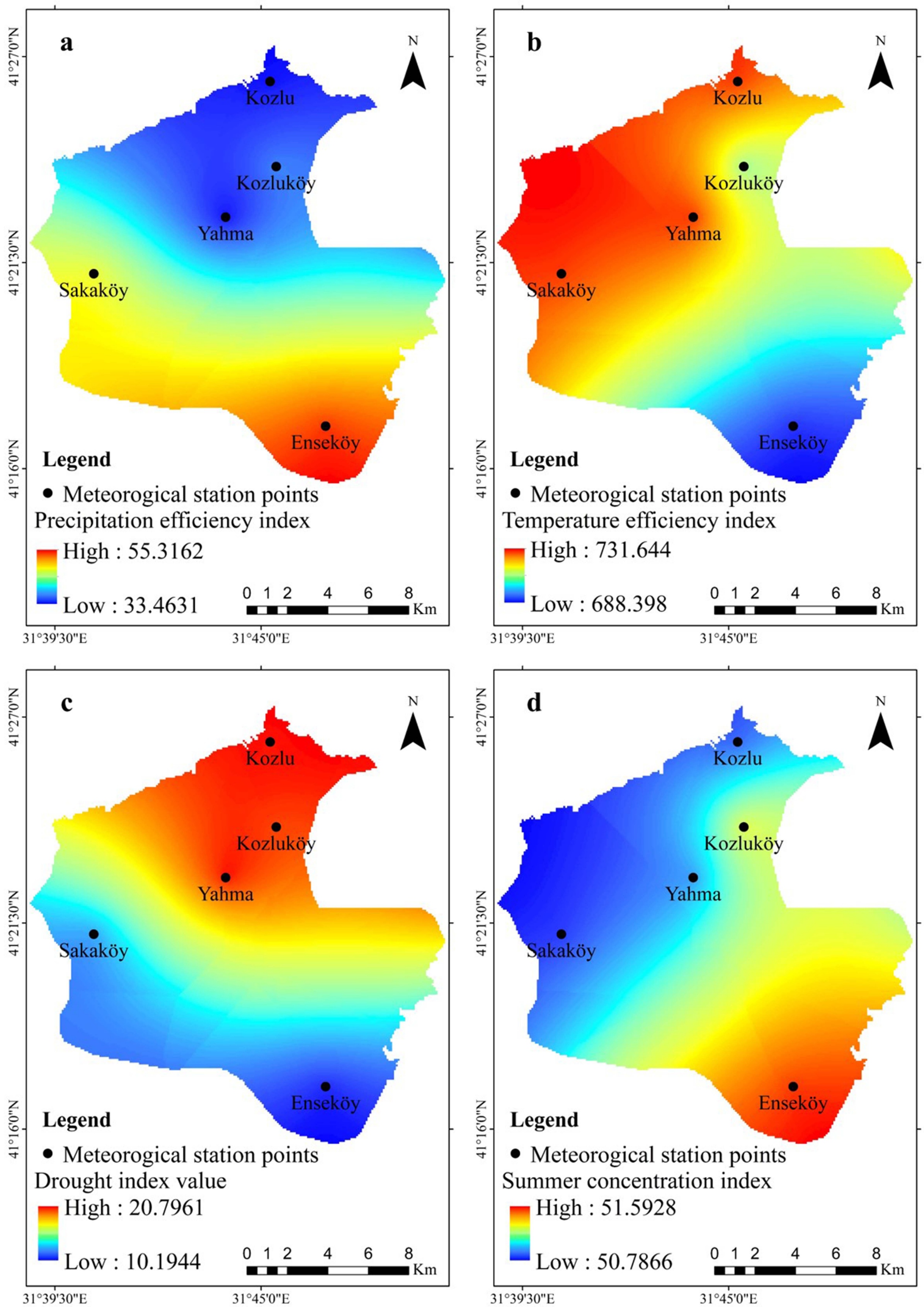


**Figure 6.** Thornthwaite based climate border maps; a) precipitation efficiency index, b) temperature efficiency index, c) drought index, and d) summer concentration index.

The Thornthwaite method is primarily used for climate classification, but it is also applicable when direct evapotranspiration calculations are not feasible. Therefore, to generate the climate map of the Kozlu, the results obtained from the Thornthwaite method representing the first, second, third, and fourth letters have been examined using the Kriging interpolation method (Krige, 1951) in GIS software. As a result of the analysis, maps representing the precipitation efficiency index (Figure 6a), temperature efficiency index (Figure 6b), drought index (Figure 6c), and summer concentration index (Figure 6d) have been prepared. This allowed for climate estimation in locations beyond the stations included in the study. By determining climate characteristics based on station data and generating raster-based maps, this study ensured a more accurate spatial determination of climate boundaries.

When comparing the climate characteristics of the Kozlu district obtained in this work with the climate maps of Turkey (Türkiye) provided by MGM (2024), it was observed that the results were consistent. Considering the presence of geo-environmental features that restrict the development of the district (Arca et al., 2017), landslide (Arca et al., 2018), subsidence (Can et al., 2011), and flood risks (Keskin Citiroglu and Baysal, 2011), along with the potential for wind energy utilization (Arca and Keskin Citiroglu, 2022), it is evident that the conclusions of this investigation will contribute to energy production, land use, disaster prevention, and various planning efforts in the Kozlu district. Transformation of undeveloped areas into urban areas can cause an increase in the effects of climate change by changing the biophysical properties of the area (Koç, 2024; Kazancı Altınok, 2022). In spatial planning studies, the protection of the city's coastal areas, agricultural, forest and wetlands is important in establishing the principles of adaptation to climate change (Kazancı Altınok, 2022). Kozlu faces many unplanned construction, rugged topography, a geological and karstic structure, mining activities, and mass movements (Arca et al., 2017). To ensure the healthy continuation of urban development in Kozlu district and the sustainability of district resources, it is important to prevent climate-related problems and to harmonize urban development with climate characteristics. Considering that climate change affects landslide formation by increasing heavy rainfall, which is the trigger of landslides (Gariano and Guzzetti 2016), it is necessary to know the climate characteristics of Kozlu district.

## 5. Conclusion

In this study, climate boundaries were determined in the Kozlu district located on the Black Sea coast to prevent both climate-related problems and potential impacts of climate. For this purpose, meteorological station data from the last thirty years in the district were used to define the climate patterns of station points according to Thornthwaite. Subsequently, surface analysis was conducted using the Kriging interpolation method. Thus, maps of the climate border reflecting the climate styles at midpoints covering the entire study area were obtained.

In the Kozlu district, precipitation is observed in all months, with an increase in October that continues until February. October and December receive more precipitation than other months in the region. Throughout the study area, the average highest temperatures are observed in July and August, while the average minimum temperatures occur in January and February. The temperature, which shows a decreasing trend in September in Kozlu, exhibits an increasing trend starting in April. As one moves southward in the Kozlu district, the annual precipitation increases, while the intensity of temperature and the duration of water deficiency decrease.

In the entire district, ETP is top in July and minimum in January. However, ETR is lowest in January across the entire district, while it is highest in June for Kozlu and Kozluköy stations, and in July for Enseköy and Sakaköy stations. Additionally, from November to May, there is excess water and surface runoff throughout the district. Some of the excess water contributes to surface runoff, while some infiltrates into the soil, with the top surface runoff occurring in February.

According to the climate classification conducted using the Thornthwaite method, a humid climate prevails throughout district, represented by the first and second letters. The drought index represented by the third letter indicates moderate summer water deficiency in the northern part of the district and little or no water deficiency in the southern part for rainy climates. Considering that the stations located in the southern part of the study area receive higher annual precipitation compared to other districts and have a shorter duration of water deficit, the observation of the little or no water deficiency climate characteristic as one moves southward in the study area demonstrates a high level of consistency among the results. According to the summer concentration index represented by the fourth letter in the Thornthwaite method, the entire investigated area displays a marine characteristic.

The results obtained are valuable for assisting in planning that is either based on climate or affected by climate as they can reveal areas where climate changes occur throughout the district. The determination of climate boundaries will facilitate the resolution of various issues in Kozlu district affected by climate characteristics such as landslides, subsidence events, floods, and land use, changes in plant species, agricultural planning, and migration problems. Mapping climate boundaries will contribute to monitoring climate change, which is as important as all these contributions. Thus, it will not only contribute to local-scale efforts but also contribute to national-scale initiatives addressing climate change.

It is evident that the outputs of this study have the potential for development and will assist decision-makers in managing climate change risks and water resources in Kozlu. Kozlu also has opportunities in mining, tourism, agriculture, and fishing. The absence of a rainless month in Kozlu ensures that plants can meet most of their water needs from rainfall. The months of autumn and winter display similar characteristics. The fact that Kozlu has a humid climate and the precipitation it has makes it possible to conduct irrigation and eliminate the time and financial losses that irrigation tends to cause. Although there is a decrease in the amount of precipitation in July, the need for irrigation in agricultural activities can be eliminated if early harvested products are grown.

Protecting water resources is mandatory for sustainable urban development. Therefore, the effects of artificial environments on surface and underground water resources, climate characteristics, and climate change scenarios must be taken into account in urban planning. With the results of this study, the climate character and climatic changes of the region should be revealed, and the Climate Model Comparison Project CMIP5 and CMIP6 scenarios should be prepared.

The Thornthwaite method allows for the determination of climate classifications and the calculation of features such as water deficiency, evapotranspiration, humidity, and runoff. In other words, its capability to be used in situations where evapotranspiration cannot be immediately determined demonstrates that the Thornthwaite method is a robust and advantageous approach. In this context, when the methods used in determining the climate type are compared, the Thornthwaite method is more detailed and reveals critical issues such as evaporation-transpiration, soil moisture level, surface flow and water requirement.

## Acknowledgements

The authors would like to thank the editors and reviewers for their review and recommendations. The authors would also like to thank Dr. Eda Çevik, a research assistant at Dokuz Eylul University Izmir Vocational School in Turkey, for her contributions in the application of the nonparametric statistical method Kruskal Wallis Test.

## Funding statement

The authors received no specific funding for this study.

## Author's contribution

Hulya Keskin Citiroglu: supervision, data curation, conceptualization, investigation, methodology, formal analysis, calculations, original draft and preparation. Deniz Arca: data curation, conceptualization, investigation, methodology, formal analysis, analysis of GIS and visualization, writing, and review. All authors reviewed the results and approved the final version of the manuscript.

## Availability of data and materials

The data that support the findings of this research are available from the author upon reasonable request.

## Conflict of competing interest

None declared.

## References

Aalto, J., Pirinen, P., Heikkinen, J., Venäläinen, A. 2013. *Spatial interpolation of monthly climate data for Finland: comparing the performance of kriging and generalized additive models*. Theor. Appl. Climatol. 112(1–2), 99–111.

Akinci, H., 2022. *Assessment of rainfall-induced landslide susceptibility in Artvin, Turkey using machine learning techniques*. J. Afr. Earth Sci. 191, 104535. https://doi.org/10.1016/j.jafrearsci.2022.104535

Arca, D., Keskin Citiroglu, H., 2022. *Geographical information systems-based analysis of site selection for wind power plants in Kozlu District (Zonguldak-NW Turkey) by multi-criteria decision analysis method*. Energy Sources Pt. A – Recovery Util. Environ. Eff. 44(4), 10720–10732. https://doi.org/10.1080/15567036.2020.1834030

Arca, D., Keskin Citiroglu, H., 2024. *Determining climate classifications and producing climate border maps with GIS of Muğla province on the southern Aegean Sea coast of Türkiye*. Theor. Appl. Climatol. 155(7), 5745–5757. https://doi.org/10.1007/s00704-024-04954-2

Arca, D., Keskin Citiroglu, H., Kutoğlu, H.S., Mekik, C., Deguchi, T., 2017. *Assessment of geo-environmental properties depressing urban development with GIS: a case study of Kozlu settlement, Turkey*. Nat. Hazards 87(1), 307–322.

Arca, D., Kutoglu, S.H., Becek, K., 2018. *Landslide susceptibility mapping in an area of underground mining using the multicriteria decision analysis method*. Environ. Monit. Assess. 190, 725. https://doi.org/10.1007/s10661-018-7085-5

Arslan, O., 2021. *Ankara ili içme suyu kalite parametrelerinin coğrafi bilgi sistemleri (CBS) ortamında farklı enterpolasyon yöntemleri kullanılarak modellenmesi*, (M.Sc. Thesis), Nevşehir Hacı Bektaş Veli Üniv., Turkey.

Bajjali, W., 2017. *ArcGIS for environmental and water issues*. Springer Int. Publ., 353 pp.

Behera, S.K., Shukla, A.K., 2015. *Spatial distribution of surface soil acidity, electrical conductivity, soil organic carbon content and exchangeable potassium, calcium and magnesium in some cropped acid soils of India*. Land Degrad. Dev. 26 (9), 71–79.

Belda, M., Holtanová, E., Halenka, T., Kalvová, J., 2014. *Climate classification revisited: From Köppen to Trewartha*.

Clim. Res. 59, 1–13. http://dx.doi.org/10.3354/cr01204

Bidinger, F.R., 1979. *Transfer of agricultural technology*. Develop. Transfer Tech., p. 71.

Bieniek, P.A., Bhatt, U.S., Thoman RL. 2012. *Climate divisions for Alaska based on objective methods*. J. Appl. Meteor. Climatol. 51, 1276–1289.

Bolat, İ., Kara, Ö., Tok, E., 2018. *Global warming and climate change: a practical study on Bartin, Zonguldak and Düzce*. J. Bartin Facult. Forestry (BAROFD) 20(1), 116–127. https://doi.org/10.24011/barofd.374840

Bostan, P., 2017. *Basic Kriging methods in geostatistics*. J. Agricult. Sci. 27(1), 10–20 (Yüzüncü Yıl Univ.).

Boz, A.Ö., Dönmez, Y., Özyavuz, M., 2020. *Use of climate maps in determining sustainable agriculture areas*. J. Environ. Protec. Ecol. 21(3), 1062–1071.

Calda, B., An, N., Turp, M.T., Kurnaz, M.L., 2020. *Effects of climate change on the wildfires in the Mediterranean Basin*. Int. J. Adv. Eng. Pure Sci. 1, 15–32. https://dx.doi.org/10.7240/jeps.571001

Camargo, A.P. de., 1991. *Classificação climática para zoneamento de aptidão agroclimática*. Rev. Brasil. Agrometeorol. 8, 126–131.

Carmin, J., Anguelovski, I., Roberts, D., 2012. *Urban climate adaptation in the global south: planning in an emerging policy domain*. J. Plan. Edu. Res. 32(1), 18–32. https://doi.org/10.1177/0739456X11430951

Can, E., Mekik, C., Kuscu, S., Akcin, H., 2011. *Subsidence occurring in mining regions and a case study of Zonguldak-Kozlu Basin*. Sci. Res. Essays. 6(6), 1317–1327.

Climate Data, 2024. *Climate data for cities around the world. Climate Data*. https://tr.climate-data.org/

Colak, H. E., Memisoglu, T., 2021. *Thornthwaite iklim sınıflandırma yöntemine göre Karadeniz Bölgesi iklim sınır haritasının CBS ile üretilmesi*. Geomatik 6(1), 31–43. https://doi.org/10.29128/geomatik.651702

Coumou, D., Rahmstorf, S.A., 2012. *Decade of weather extremes*. Nat. Clim. Change 2(7), 491–496.

Cui, D., Liang, S., Wang, D., 2021. *Observed and projected changes in global climate zones based on Köppen climate classification*. WIREs Clim. Change 12:e701. https://doi.org/10.1002/wcc.701

de Castro, M., Gallardo, C., Jylha, K., Tuomenvirta, H., 2007. *The use of a climate-type classification for assessing climate change effects in Europe from an ensemble of nine regional climate models*. Clim. Chang. 81 (Suppl. 1), 329–341. https://doi.org/10.1007/s10584-006-9224-1

de Oliveira Aparecido, L.E., de Meneses, K.C., Lorençone, P.A. et al., 2023. *Climate classification by Thornthwaite (1948) humidity index in future scenarios for Maranhão State, Brazil*. Environ. Dev. Sustain. 25, 855–878. https://doi.org/10.1007/s10668-021-02082-9

Elguindi, N., Grundstein, A., Bernardes, S., Turuncoglu, U., Feddema, J., 2014. *Assessment of CMIP5 global model simulations and climate change projections for the 21st century using a modified Thornthwaite climate classification*. Clim. Chang. 122, 523–538. https://doi.org/10.1007/s10584-013-1020-0

Erinç, S., 1984. *Klimatoloji ve metodları*. I.U. Publ. 3278, Deniz Bilimleri ve Coğ. Enst. 2, Istanbul.

Flohn, H., 1950. *Neue Anschauungen über die allgemeine zirkulation der atmosphareund ihre klimatische bedeutung*. Erdkunde 4, 141–162.

Gallardo, C., Gil, V., Hagel, E., Tejeda, C., Castro, M., 2013. *Assessment of climate change in Europe from an ensemble of regional climate models by the use of Köppen–Trewartha classification*. Int. J. Climatol. 33, 2157–2166.

Gariano, S.L., Guzzetti, F., 2016. *Landslides in a changing climate*. Earth-Sci. Rev. 162, 227–252.

Gregory, W.L., Duran, A., 2001. *Scenarios and acceptance of forecasts*. [in:] *Principles of forecasting: a handbook for researchers and practitioners*. J. Scott Armstrong (ed.), Springer Sci., Business Media Inc., New York.

Gürkan, H., Arabaci, H., Demircan, M., Eskioğlu, O., Şenso, S., Yazici, B., 2016. *Temperature and precipitation projections based on GFDL-ESM2M using RCP4.5 and RCP8.5 scenarios for Turkey*. Coğrafi Bilimler Dergisi CBD 14 (2), 77–88.

Holdridge, L.R., 1967. *Life zone ecology*. Tropical Science Center, San Jose, Costa Rica, 266 pp.

IPCC, 2013. Climate change 2013. *The Physical Science Basis*. Working Group I Contribution to the Fifth Assessment Report of the Intergovernmental Panel on Climate Change, Cambridge Univ. Press, England.

IPCC, 2000. Special report on emissions scenarios. Cambridge University Press, England.

Işlem GIS., 2005. *ArcGIS 9 uygulama dökümanı*. İşlem Coğrafi Bilgi Sistemleri Mühendislik ve Eğitim Ltd. Şti. Sinan Ofset Matbaacılık, Ankara.

Jacobeit, J., 2010. *Classifications in climate research*. Phys. Chem. Earth 35, 411–421.

Jylhä, K., Tuomenvirta, H., Ruosteenoja, K., Niemi-Hugaerts, H., Keisu, K., Karhu, J.A., 2010. *Observed and projected future shifts of climatic zones in Europe and their use to visualize climate change information*. Weather Climate Soc. 2, 148–167. https://doi.org/10.1175/2010WCAS1010.1

Kazancı Altınok, G., 2022. *Kentsel büyüme dinamiklerinin iklim değişikliği etkileri çerçevesinde yeniden irdelenmesi*. Çevre Şehir Ve İklim Dergisi 1(1), 174–198.

Keskin Citiroglu, H., 2024. *Determining climate classifications and producing climate border maps with GIS of Safranbolu district, Karabük, Türkiye*. Environ. Monit. Assess. 196, 402. https://doi.org/10.1007/s10661-024-12562-w

Keskin Çıtıroğlu, H., Arca, D., 2024. *Bartın ilinin iklim sınıflarının belirlenmesi ve CBS tabanlı iklim sınır haritalarının oluşturulması*. Doğ. Afet. Çev. Derg. 10(2), 282–294.
https://doi.org/10.21324/dacd.1427198

Keskin Citiroglu, H., Baysal, G., 2011. *Effects of geological and hydrological factors on the creation of flooding in Kozlu, Zonguldak, NW Turkey*. Int. J. Physic. Sci. 6(6), 1360–1373.

Koç, C., 2024. *Kentsel büyüme ve iklim değişikliğinin Yalova örneğinde değerlendirilmesi*. DÜFED 13, 11–44.
https://doi:10.55007/dufed.1246371

Kozlu District Governorship, 2024. *Kozlu*.
http://www.kozlu.gov.tr/ilcemiz

Kozlu Municipality, 2024. *Life in Kozlu*.
https://www.kozlu.bel.tr/kozluda-yasam

Köppen, W., Geiger, R., 1928. *Klimate der Erde, Justus Perthes, Gotha*.

Krige, D.G., 1951. *A statistical approach to some mine valuations and Witwatersrand*. Witwatersrand.

Lakshmi, R., Thomas, J., Joseph, S., 2024. *Impacts of recent rainfall changes on agricultural productivity and water resources within the Southern Western Ghats of Kerala, India*. Environ. Monit. Assess. 196, 115.
https://doi.org/10.1007/s10661-023-12270-x

Mahlstein, I., Daniel, J.S., Solomon, S., 2013. *Pace of shifts in climate regions increases with global temperature*. Nat. Clim. Chang. 3, 739–743.

MGM, 2024. *Climate classification, Zonguldak*. Ministry of Environment, Urbanization and Climate Change, General Directorate of Meteorology.
https://www.mgm.gov.tr/iklim/iklim-siniflandirmalari.aspx?m=ZONGULDAK

MGM, 2025. *Klimatoloji-II*. Ministry of Environment, Urbanization and Climate Change, General Directorate of Meteorology.
https://www.mgm.gov.tr/FILES/iklim/klimatoloji2.pdf

Orhan, O., Dadaser-Celik, F., Ekercin, S., 2019. *Investigating land surface temperature changes using Landsat-5 data and real-time infrared thermometer measurements at Konya Closed Basin in Turkey*. Int. J. Eng. Geosci. (IJEG) 4(1), 16–27.
https://doi.org/10.26833/ijeg.417151

Özüpekçe, S., 2021. *Drought analysis and relationship with water resources of Western Mediterrenean Basins closed area*. Int.J. Geogr. & Geogr. Edu. IGGE 43, 317–337.

Rahimi, J., Ebrahimpour, M., Khalili, A., 2013. *Spatial changes of extended De Martonne climatic zones affected by climate change in Iran*. Theor. Appl. Climatol. 112, 409–418.

Rolim, G. de S., Paes, de Camargo M.B., Lania, D.G., Leite de Moraes, J.F., 2007. *Climatic classification of Köppen and Thornthwaite sistems and their applicability in the determination of agroclimatic zonning for the state of São Paulo, Brazil*. Bragantia 66(4), 711–720.

Santos, C.N., Santos, A.A.R., Abreu, M.C. et al., 2024. *Monthly potential evapotranspiration estimated using the Thornthwaite method with gridded climate datasets in Southeastern Brazil*. Theor. Appl. Climatol. 155, 3739–3756.
https://doi.org/10.1007/s00704-024-04847-4

Schendel, U., 1968. *Messungen mit grundwasser lysimeter über den wasserverbrauch aus oberflachennahem grunwasser*. Z. Grundwasser 9, Kulturtechnik Flurbereich, Berlin//Hamburg, 314–326.

Schmidt, S., 2010. *Kruskal–wallis test*. [in:] *Encyclopedia of Research Design*, 674–676. SAGE Publ. Inc.
https://doi.org/10.4135/9781412961288

Shanmugam, M., Lim, S., Hosan, M.L., Shrestha, S., Babel, M. S., Virdis, S.G.P., 2024. *Lapse rate-adjusted bias correction for CMIP6 GCM precipitation data: An application to the Monsoon Asia Region*. Environ. Monit. Assess. 196, 49.
https://doi.org/10.1007/s10661-023-12187-5

Singh, P., Khan, I., 2011. *Ground water quality assessment of Dhankawadi ward of Pune by using GIS*. Int. J. Geomatics Geosci. (IJGAGS), 688–703.

Spinoni, J., Vogt, J., Naumann, G., Carrao, H., Barbosa, P., 2014. *Towards identifying areas at climatological risk of desertification using the Köppen–Geiger classification and FAO aridity index*.
Int. J. Climatol. 35, 2210–2222.

Taylan, E.D., Damçayırı, D., 2016. *Isparta Bölgesi Yağış değerlerinin IDW ve Kriging Enterpolasyon Yöntemleri ile tahmini*. İMO Teknik Dergi. 459.

Taylor, K. E., Stouffer, R. J., Meehl, G. A., 2012. *An overview of CMIP5 and the experiment design*. Bull. Am. Meteorol. Soc. (BAMS) 93(4), 485–498.
https://doi.org/10.1175/BAMS-D-11-00094.1

Thornthwaite, C.W., 1948. *An approach toward a rational classification of climate*. Geogr. Rev. 38(1), 55–94.

TUIK, 2024. *Address based population census*. Türkiye İstatistik Kurumu.
https://www.tuik.gov.tr/

URL-1, 2024. *Türkiye mülki idare haritaları*. Coğrafya-Harita.
http://cografyaharita.com/haritalarim/4l-zonguldak-ili-haritasi.png

Uyan, M., Cay, T., 2013. *Spatial analyses of groundwater level differences using geostatistical modeling*. Environ. Ecol. Stat. 20(4), 633–646.

Üstüntaş, T., 2006. *Sayısal arazi modellerinde bazı enterpolasyon yöntemlerinin karşılaştırılması*. Selçuk Univ. Tech., Voc. School Tech. Sci. 5(2), 41–48 (online).

Valjarević, A., Milanović, M., Gultepe, I., Filipović, D., Lukić, T., 2022. *Updated Trewartha climate classification with four climate change scenarios*. Geogr. J. 188, 506–517.
https://doi.org/10.1111/geoj.12458

Van Delden, H., Stuczynski, T., Ciaian, P., Paracchini, M.L., Hurkens, J., Lopatka, A., Shi, Yu-e., Prieto, O.G., Calvo, S., van Vliet, J., Vanhout, R., 2010. *Integrated assessment of agricultural policies with dynamic land use change modelling*. Ecol. Modell. 221(18), 2153–2166.

Yalcin, F., Arca, D., 2024. *Investigation and comparison of climate boundary maps generated with various climate classifications*. [in:] *Interdisciplinary studies on contemporary research practices in engineering in the 21st century*, K. Kaygusuz (ed.), Gaziantep, Ozgur Press, 33–88.

Yaprak, S., Arslan, E., 2008. *Kriging yöntemi ve geoit yüksekliklerinin enterpolasyonu. Jeodezi, Jeeinformasyon ve Arazi Yönetimi Dergisi*, JGG 1(98), 36–42.

Yılmaz, G., 2023. *Kuraklık ve sıcak hava dalgasının tarımsal üretim üzerine etkileri*. Doğ. Afet. Çev. Derg. 9(2), 240–257. https://doi.org/10.21324/dacd.1220462